

1 Hamiltonian dynamics of thermostated systems: Two-temperature 2 heat-conducting ϕ^4 chains

3 Wm. G. Hoover^{a)} and Carol G. Hoover

4 Highway Contract 60, Ruby Valley, Nevada 89833 and HiTech Center, Great Basin College,
5 Elko, Nevada 89801

6 (Received 31 January 2007; accepted 7 March 2007)

7 We consider and compare four Hamiltonian formulations of thermostated mechanics, three of them
8 kinetic, and the other one configurational. Though all four approaches “work” at equilibrium, their
9 application to many-body nonequilibrium simulations can fail to provide a proper flow of heat. All
10 the Hamiltonian formulations considered here are applied to the same prototypical two-temperature
11 “ ϕ^4 ” model of a heat-conducting chain. This model incorporates nearest-neighbor Hooke’s-Law
12 interactions plus a quartic tethering potential. Physically correct results, obtained with the isokinetic
13 Gaussian and Nosé-Hoover thermostats, are compared with two other Hamiltonian results. The latter
14 results, based on constrained Hamiltonian thermostats, fail to model correctly the flow of heat.
15 © 2007 American Institute of Physics. [DOI: 10.1063/1.2720839]
16

17 I. INTRODUCTION

18 Computational “thermostats” arose as a means for con-
19 trolling numerical simulations of both equilibrium and non-
20 equilibrium stationary states. *Without* thermostats systems
21 driven away from equilibrium heat up. *With* thermostats the
22 heat generated by irreversible processes can be steadily re-
23 moved, making it possible to simulate nonequilibrium steady
24 states.^{1,2} Because most Hamiltonian-based mechanics prob-
25 lems conserve energy, novel *nonHamiltonian* ideas are typi-
26 cally required when thermostats are to be included. Never-
27 theless, several approaches to Hamiltonian thermostats have
28 been developed. Here we consider various approaches pio-
29 neered by Ashurst, Dettmann, Evans, Hoover, Leete, Mor-
30 riss, Nosé, and Woodcock over a span of about 25 years.^{1–10}

31 The simplest thermostat type maintains a (nearly) con-
32 stant kinetic energy by “rescaling” the velocities at the end of
33 each computational time step. For a more elegant, but
34 equivalent, *continuous* approach to rescaling, see the “Gauss-
35 ian isokinetic” method described in Sec. II B and illustrated
36 in Sec. VII. For # Cartesian degrees of freedom the kinetic-
37 theory relation

$$38 \quad K = \sum \frac{m\dot{q}^2}{2} = \sum \frac{p^2}{2m} = \# \frac{kT_{\text{kin}}}{2},$$

39 defines the kinetic temperature T_{kin} . Thermostats based on
40 T_{kin} can be applied to an entire system, or separately to two
41 or more subsystems. With this *ad hoc* rescaling approach

$$42 \quad p \rightarrow p_0 \sqrt{(K/K_0)},$$

43 there is no difficulty in maintaining several temperatures in
44 specified parts of a single nonequilibrium system, as did
45 Ashurst in his Ph.D. thesis research.¹¹

The kinetic theory and the Gibbs-Boltzmann develop- 46
ment of thermodynamics based on ideal-gas thermometry 47
certainly suggest that the kinetic temperature, T_{kin} , is both 48
the simplest and the most fundamental of the many possible 49
“temperature” types. There are alternatives. Among the many 50
possible temperatures based on particle coordinates, rather 51
than velocities, the simplest—on which we focus here—is 52
based on the mean-squared forces, $\langle F^2 \rangle$. This definition of a 53
configurational temperature is derived directly from the po- 54
tential energy Φ and its space derivatives 55

$$56 \quad kT = \langle (\nabla\Phi)^2 \rangle / \langle \nabla^2\Phi \rangle = - \langle F^2 \rangle / \langle \nabla F \rangle.$$

This somewhat cumbersome relation appears as an aside in 57
Landau and Lifshitz’ classic 1958 text.¹² It was also recently 58
rediscovered by Rugh, and has subsequently been much 59
discussed.^{13–16} This configurational representation of tem- 60
perature follows most simply from an integration by parts, in 61
the canonical ensemble: 62

$$63 \quad \int dq \nabla^2 \Phi = \nabla \Phi; \quad (-d/dq) e^{-\Phi/kT}$$

$$64 \quad = (\nabla\Phi/kT) e^{-\Phi/kT} \rightarrow \int dq \nabla^2 \Phi e^{-\Phi/kT}$$

$$65 \quad = (1/kT) \int dq (\nabla\Phi)^2 e^{-\Phi/kT}.$$

About ten years after Woodcock and Ashurst’s introduction 66
of the rescaling isokinetic thermostat in the early 1970s, 67
Hoover and Evans discovered that the isokinetic velocity- 68
rescaling equations of motion can be derived from Gauss’ 69
Principle of Least Constraint.⁵ Fifteen years after this discov- 70
ery, Dettmann and Morriss⁴ found a straightforward Hamil- 71
tonian approach to these same motion equations. Previously, 72
Leete and Hoover had derived a Hamiltonian formulation 73
which likewise maintained the velocity-based kinetic energy 74
 $K(\{\dot{q}\})$ constant.^{6,8} 75

^{a)}Author to whom correspondence should be addressed. Electronic mail:
hooverwilliam@yahoo.com

76 A Hamiltonian generating the Gauss' principle isokinetic
77 equations of motion was not found until 1996.⁴ In the mean-
78 time Nosé had discovered his canonical-ensemble thermo-
79 stated dynamics, which is related to two rather different
80 Hamiltonians.^{7,9} The purpose of the present work is twofold.
81 First, we explore the relation of the Hoover-Leete kinetic
82 thermostat work to its successors. A 2007 literature search
83 shows only a single reference to it.⁶ We also explore the
84 consequences of a "Landau-Lifshitz" configurational thermo-
85 stat based on the canonical-ensemble definition rediscovered
86 by Rugh with a relatively complicated measure-based ap-
87 proach using the *microcanonical* ensemble. Recent peda-
88 gogical reviews of this configurational-temperature work can
89 be found in Refs. 13–16.

90 II. THE NOSÉ-HOOVER THERMOSTAT

91 The Nosé-Hoover equations of motion^{1,9} are a standard
92 approach to carrying out canonical-ensemble dynamics at a
93 particular temperature T_0 . This approach uses *feedback*, con-
94 trolling the fluctuating kinetic energy with a "friction coeffi-
95 cient" or "control variable" ζ . The frictional feedback force
96 is $-\zeta p$. The time rate of change of the friction coefficient is
97 based on the current value of the kinetic energy $K(t)$ relative
98 to the desired mean value $K_0(T_0)$. The equations of motion
99 also include a characteristic time τ which determines the
100 time-range over which the feedback acts

$$101 \quad \{\dot{q} = p/m; \quad \dot{p} = F - \zeta p\}; \quad \dot{\zeta} = [(K/K_0) - 1]/\tau^2.$$

102 It is quite interesting to see that a canonical-ensemble
103 approach¹ to a Nosé-Hoover-type *configurational* thermostat
104 led Braga and Travis¹⁴ to the motion equations (for a har-
105 monic oscillator with unit mass, force constant, and tempera-
106 ture)

$$107 \quad \dot{q} = p - \zeta q; \quad \dot{p} = -q; \quad \dot{\zeta} = [q^2 - 1]/\tau^2.$$

108 The substitution $(+q, +p, +\zeta, +t) \rightarrow (-p, -q, -\zeta, -t)$ gives

$$109 \quad \dot{p} = -q - \zeta p; \quad \dot{q} = +p; \quad \dot{\zeta} = [p^2 - 1]/\tau^2,$$

110 *exactly* the same as the Nosé-Hoover equations for the *ki-*
111 *netic* thermostating of an oscillator!

112 In most cases, including our ϕ^4 model studies described
113 in detail in Secs. V–IX, a reasonable choice of τ corresponds
114 to a typical collision time or vibration time. Such a choice
115 typically provides the Gibbs' equilibrium canonical phase-
116 space distribution with a Gaussian distribution for the fric-
117 tion coefficient ζ

$$118 \quad f(q, p, \zeta) = e^{-\Phi/kT} e^{-K/kT} e^{-\# \zeta^2 \tau^2/2}.$$

119 Evidently the amplitude of the fluctuations of ζ varies as
120 $\sqrt{1/\# \tau^2}$, where $\#$ is the number of degrees of freedom. Thus
121 its effect on the dynamics vanishes in the large-system limit.

122 *Nonequilibrium* situations are quite different. By using
123 two or more different friction coefficients (or "thermostat
124 variables") temperature differences can be established, lead-
125 ing to heat flow. Then the corresponding phase-space distri-
126 butions are no longer smooth and Gibbsian, but instead be-
127 come fractal, with the underlying phase-space trajectories

satisfying the second law of thermodynamics infinitely more
probable than those violating the law.² In the equilibrium
case there is a close connection of Nosé-Hoover mechanics
to Hamiltonian mechanics. We describe this connection next.

A. The Dettmann-Nosé Hamiltonian

In 1984 Nosé discovered a Hamiltonian consistent with
Gibbs' constant-temperature canonical ensemble

$$f(q, p) \propto \exp(-\mathcal{H}_{\text{Nosé}}/kT).$$

He was able to derive the Nosé-Hoover equations of motion
described above from his Hamiltonian by an artificial "time
scaling."

In July of 1996 Dettmann⁷ discovered a simpler ap-
proach to the Nosé-Hoover equations of motion. Dettmann's
vanishing Hamiltonian is

$$\mathcal{H}_{\text{Dettmann}} \equiv s\mathcal{H}_{\text{Nosé}} = \sum \frac{p^2}{2ms} + s \left[\Phi + \frac{p_s^2}{2M} + \# kT \ln s \right] \equiv 0.$$

Provided that Dettmann's Hamiltonian is set equal to the
special value, zero, Nosé's time-scaling variable s can be
eliminated. Then the Nosé-Hoover equations of motion result
without the need for any time scaling. It needs to be empha-
sized that this $\mathcal{H}=0$ trick does *not* work for the prototypical
nonequilibrium case of a system with two different tempera-
tures. In a two-temperature system the two different vari-
ables $s_{\text{Hot/Cold}}$ are necessarily coupled and cannot both be
eliminated, so that Dettmann's $\mathcal{H}=0$ trick does not work.

There is a special case of Nosé-Hoover dynamics that
deserves special mention, the "isokinetic" case in which the
temperature is constant. This corresponds to the choice τ
 $\rightarrow 0$. For isokinetic mechanics Dettmann and Morris discov-
ered the special Hamiltonian detailed next.

B. The Dettmann-Morriss isokinetic Hamiltonian

Soon after Dettmann discovered a Hamiltonian route to
the Nosé-Hoover motion equations, Dettmann and Morriss⁴
discovered a related approach to isokinetic (constant tem-
perature, provided that temperature is defined by the kinetic
energy) Hamiltonian dynamics

$$\mathcal{H}_{\text{DM}} = Ke^{+\Phi/2K_0} - K_0 e^{-\Phi/2K_0} \equiv 0; \quad K \equiv \sum \frac{p^2}{2m}.$$

As usual, the equations of motion follow by differentiation

$$\{\dot{q} = \partial\mathcal{H}/\partial p = pe^{+\Phi/2K_0}; \quad \dot{p} = -\partial\mathcal{H}/\partial q = Fe^{-\Phi/2K_0}\}.$$

The accelerations which follow, using the identity

$$K/K_0 = e^{-\Phi/K_0},$$

are then exactly the same as those from the isokinetic equa-
tions of motion given above

$$170 \quad \{\ddot{q} = (F/m) - p \sum (F \cdot \dot{q}/2K_0)e^{+\Phi/2K_0} = (F/m) - \zeta\dot{q}\};$$

$$171 \quad \zeta = \sum F \cdot \dot{q}/(2K_0).$$

172 III. THE HOOVER-LEETE ISOKINETIC THERMOSTAT 173 IN ITS LAGRANGIAN AND HAMILTONIAN 174 FORMS

175 The Hamiltonians corresponding to the isokinetic
176 Gauss' Principle and Nosé-Hoover velocity-based ap-
177 proaches are not the only such means of thermostating equi-
178 librium systems. A straightforward application of nonholo-
179 nomic Lagrangian mechanics, as well as the familiar
180 Hamiltonian mechanics outlined in Leete's Master's thesis,⁶
181 lead to another type of isokinetic mechanics. These two
182 equivalent forms of mechanics, both of which can be used to
183 keep the *velocity*-based kinetic energy $K(\dot{q})$ constant, while
184 allowing the momentum-based kinetic energy $K(p)$ to vary,
185 proceed by modifying the $\{\dot{q}\}$, rather than the $\{p\}$, equations.
186 To distinguish the two different kinetic energies we use
187 the notation

$$188 \quad K(\dot{q}) = \sum \frac{m\dot{q}^2}{2}; \quad K(p) = \sum \frac{p^2}{2m}.$$

189 Let us begin with the Lagrangian case

$$190 \quad \mathcal{L}_{\text{HL}} \equiv K(\dot{q}) - \Phi + \lambda[K(\dot{q}) - K_0],$$

191 where $K(\dot{q})$ is the *velocity*-based kinetic energy, $\Sigma(m/2)\dot{q}^2$,
192 and the Lagrange multiplier λ has the task of maintaining
193 $K(\dot{q})$ at its initial value, K_0 , as the motion proceeds.
194 Lagrange's equations of motion follow from the usual text-
195 book differentiations of the Lagrangian with respect to the
196 velocities and coordinates:

$$197 \quad \left\{ p = \frac{\partial \mathcal{L}_{\text{HL}}}{\partial \dot{q}} = m\dot{q}(1 + \lambda); \right.$$

$$198 \quad \left. \dot{p} = m\ddot{q}(1 + \lambda) + m\dot{q}\dot{\lambda} = \frac{\partial \mathcal{L}_{\text{HL}}}{\partial q} \equiv F \right\}.$$

199 Now multiply the \dot{p} equation by \dot{q} and sum

$$200 \quad \sum m\ddot{q}(1 + \lambda)\dot{q} + \sum m\dot{q}\dot{\lambda}\dot{q} = 0 + 2K_0\dot{\lambda}$$

$$201 \quad = \sum F \cdot \dot{q} \equiv -\dot{\Phi}.$$

202 The value of the Lagrange multiplier λ follows:

$$203 \quad \lambda = \frac{(\Phi_0 - \Phi)}{2K_0} = \frac{\sqrt{4K(p)K_0} - K_0}{2K_0} = \frac{2K_0(1 + \lambda) - 2K_0}{2K_0} = \lambda,$$

204 where the last expression, which completes the identity, fol-
205 lows from the Hamiltonian given just below.

206 With Leete's help, Hoover discovered, in 1979, that the
207 *velocity*-based kinetic energy $K(\dot{q})$ can alternatively be kept
208 constant by using the (constant in time) Hoover-Leete
209 Hamiltonian

$$\mathcal{H}_{\text{HL}} \equiv \sum \dot{q}p - \mathcal{L}_{\text{HL}} = \sqrt{4K_0K(p)} + \Phi - K_0 \quad 210$$

$$= \mathcal{H}_0 = \Phi_0 + K_0, \quad 211$$

where Φ is again the usual potential energy and Φ_0 is its
initial value. 212
213

The constancy of the kinetic energy is easy to see. The
equations of motion 214
215

$$\left\{ \dot{q} = \frac{\partial \mathcal{H}}{\partial p}; \quad \dot{p} = -\frac{\partial \mathcal{H}}{\partial q} \right\} \rightarrow \left\{ \dot{q} = \frac{p}{m} \sqrt{\frac{K_0}{K(p)}}; \quad \dot{p} = F(q) \right\}, \quad 216$$

imply that the velocity-based kinetic energy does not vary 217

$$K(\dot{q}) = \frac{m}{2} \sum \dot{q}^2 = \sum \frac{p^2}{2m} \left[\frac{K_0}{K(p)} \right] \equiv K_0. \quad 218$$

At the same time, except in the equilibrium case with a large
number of degrees of freedom, there is no guarantee that the
momentum-based kinetic energy $K(p)$ is similar in magni-
tude to K_0 . But, provided that $\{m\dot{q}=p\} \rightarrow K(p) = K(\dot{q}) = K_0$ ini-
tially, Leete's equations of motion do match the Gaussian
isokinetic ones to second order 219
220
221
222
223
224

$$\left\{ \ddot{q} = \frac{F}{m} - \zeta\dot{q} \right\}; \quad \zeta = \frac{\sum F \cdot \dot{q}}{2K_0}, \quad 225$$

through the second derivatives, $\{\ddot{q}\}$, but differ in the *third*
derivatives, where the mean-squared constraint force in the
isokinetic case is less than the Hoover-Leete analog, in ac-
cordance with Gauss' Principle of Least Constraint.^{1,5} 226
227
228
229

The constraint of constant temperature in Hamiltonian
mechanics contradicts the thermodynamic notion that the en-
ergy and temperature cannot be varied independently in a
system of fixed composition and volume. Both E and T are
constants of the motion, using Leete's approach. Provided
that the initial conditions are wisely chosen, with E and T
corresponding to the *same* thermodynamic state, this ap-
proach *can* certainly be used to determine equilibrium prop-
erties. We will see, in Sec. VIII, what the (rather strange)
consequences of this thermostat are away from equilibrium. 230
231
232
233
234
235
236
237
238
239

IV. LANDAU-LIFSHITZ' CONFIGURATIONAL THERMOSTAT 240 241

A (much) more complicated Hamiltonian thermostat,
conserving the force-based *configurational* temperature T_{con} ,
can be based on straightforward (though quite tedious) holo-
nomic Hamiltonian mechanics. A proper configurationally
thermostated Hamiltonian conserves not only the Hamil-
tonian but also the configurational temperature 242
243
244
245
246
247

$$kT_{\text{con}} \equiv \sum_N F_i^2 / \sum_N \nabla_i^2 \mathcal{H}. \quad 248$$

Here k is Boltzmann's constant, which we set equal to unity
in the numerical work. A molecular dynamics simulation
based on this definition of temperature follows standard
Hamiltonian mechanics, as the temperature constraint is just
a (complicated) holonomic (coordinates only) constraint. The
simplest procedure begins with the system Lagrangian, aug-
mented with a Lagrange multiplier λ which constrains 249
250
251
252
253
254
255

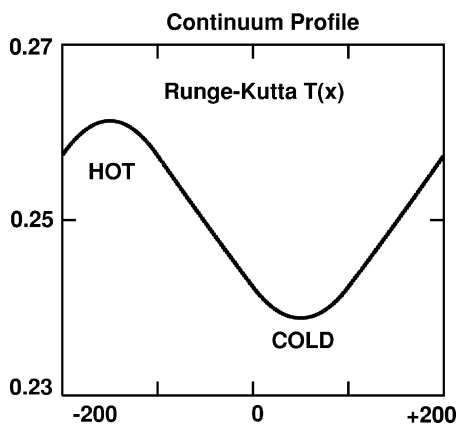


FIG. 1. Temperature profile according to Fourier's law, with mean reservoir temperatures of 0.26 ($-200 < x < -100$) and 0.24 ($0 < x < 100$).

ration d equal to unity. We also choose the strength of the Hooke's-Law interaction μ and the particle mass equal to unity. As was abundantly demonstrated by Aoki and Kusnezov, the combination of a site-based tethering potential with a Hooke's-Law pair potential provides the usual Fourier conductivity, with the heat flux proportional to the (sufficiently small) temperature gradient. In what follows we apply four different thermostat constraints to this potential model, using four different dynamical approaches: Nosé-Hoover, Gaussian isokinetic, Hoover-Leete isokinetic, and the Landau-Lifshitz isoconfigurational.

A numerical solution of the heat flow equation for the one-dimensional chain

$$\dot{T} = \nabla(3T^{-4/3} \nabla T) \pm \alpha T, \quad (303)$$

can be obtained by Runge-Kutta integration, with a rescaling of the temperatures within the reservoir regions at the end of each time step accounting for the source and sink terms in the flow equation. Figure 1 shows a fully converged temperature profile obtained in this way, using hot and cold temperatures of 0.26 and 0.24, with 400 mesh points. The spatial gradient operations were replaced by finite-difference approximations

$$(\nabla T)_i = (T_{i+1} - T_{i-1})/2, \quad (312)$$

with appropriate subscript changes accounting for the periodic boundary conditions.

VI. RESULTS WITH THE NOSÉ-HOOVER THERMOSTAT

With a periodic system composed of four parts, "Hot," "Newton₁," "Cold," and "Newton₂," each part containing $N/4$ particles, the equations of motion are

$$\{m\ddot{q} = F - \zeta_{\text{Hot}}m\dot{q}\}; \quad \dot{\zeta}_{\text{Hot}} = [(K/K_{\text{Hot}}) - 1]/\tau^2, \quad (320)$$

$$\{m\ddot{q} = F - \zeta_{\text{Cold}}m\dot{q}\}; \quad \dot{\zeta}_{\text{Cold}} = [(K/K_{\text{Cold}}) - 1]/\tau^2, \quad (321)$$

in the hot and cold regions, and

$\{T_{\text{con}}, \dot{T}_{\text{con}}, \ddot{T}_{\text{con}}\}$. The corresponding Hamiltonian has the form

$$\mathcal{H} = \Phi(\{q\}) + K(\{p\}) + \lambda(T_{\text{con}} - T_0). \quad (258)$$

For success, the initial conditions have to be chosen to correspond to both the desired temperature, $T_{\text{con}} = T_0$, and to the condition $\dot{T}_{\text{con}} = 0$. Then, to begin the analytic work, differentiate the temperature equation, $T_{\text{con}}(\{q\}) = T_0$, twice with respect to time. The two time differentiations, using the chain rule, give first $\{\dot{q}\}$ and then $\{\ddot{q}\}$. By substituting the constrained equations of motion

$$\{m\ddot{q}_i = \dot{p}_i = F_i(\{q\}) - \lambda \nabla_i T_{\text{con}}\}, \quad (266)$$

for the $\{\ddot{q}\}$, we obtain the Lagrange multiplier λ . For further details of this calculation, see Sec. IX. The numerical work can be checked by noting that both $T = T_{\text{con}}$ and \mathcal{H} are constants of the motion when the calculation is error free.

V. AOKI AND KUSNEZOV'S ϕ^4 MODEL FOR HEAT CONDUCTION

The ϕ^4 model gets its name from the functional form of a quartic "tethering potential," Φ_{Teth} , which links each particle to a fixed lattice site with a cubic restoring force

$$\Phi_{\text{Teth}} \equiv \sum_N \left(\frac{\kappa \delta^4}{4} \right) \rightarrow F_{\text{Teth}} = -\kappa \delta^3. \quad (276)$$

In the pedagogical simulations which follow we will choose the tethering force constant equal to unity, $\kappa = 1$. Nearest-neighbor particle pair interactions in the ϕ^4 model are governed by Hooke's Law

$$\Phi_{\text{Pair}} = \sum_{\text{NN}} (\mu/2)(|r| - d)^2. \quad (281)$$

Aoki and Kusnezov have carried out a variety of pedagogical heat flow simulations for this model in both one and three space dimensions.^{17,18} The ϕ^4 model has a finite Fourier conductivity in one dimension. The numerical work carried out by Aoki and Kusnezov established the temperature dependence of the thermal conductivity, $3/T^{4/3}$.

For simplicity in the one-dimensional work which we carry out here, we always choose the nearest-neighbor separation

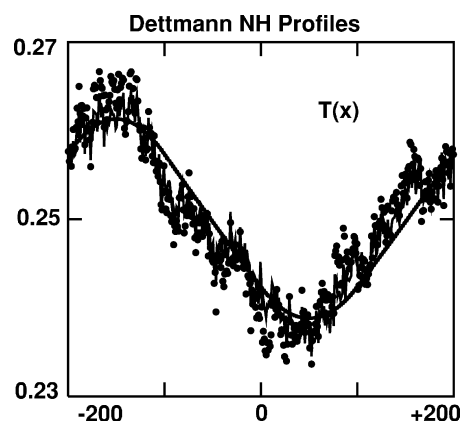


FIG. 2. Temperature profile for a conventional two-temperature Nosé-Hoover simulation, as described in the text. Here, and in the following figures, the kinetic temperature is indicated by a (quite wiggly) line, while the configurational temperature is indicated by filled circles.

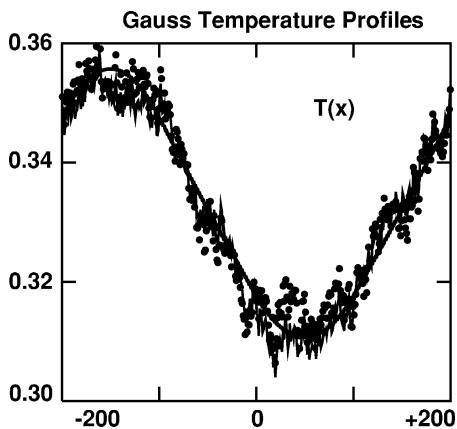


FIG. 3. Temperature profile for a conventional two-temperature Gaussian isokinetic simulation, as described in the text. The kinetic temperature corresponds to the wiggly line; the configurational temperature to the filled circles.

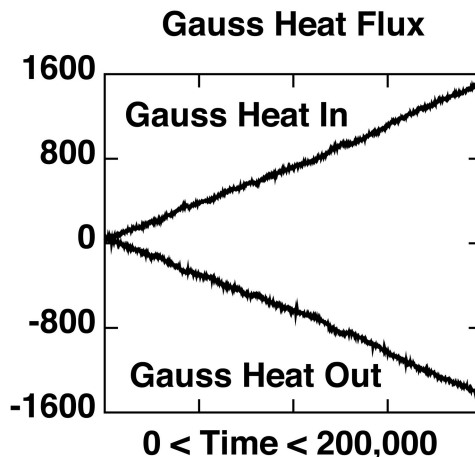


FIG. 4. Summed-up values of the heat transferred to the hot and cold Gaussian isokinetic reservoirs for the simulation of Fig. 3.

323 $\{m\ddot{q} = F\},$

324 in the two Newtonian regions. The ϕ^4 force F_i depends upon
325 the three coordinates $\{x_{i-1}, x_i, x_{i+1}\}$ and also includes the teth-
326 ering force, $F_{Teth} = -\kappa(x_i - x_0)^3$, where x_0 is the lattice site for
327 the i th particle in the perfect lattice. The initial velocities and
328 displacements were selected randomly within ranges

329 $-\Delta_v < \{v\} < +\Delta_v; \quad -\Delta_q < \{\delta q\} < +\Delta_q,$

330 with Δ_v or Δ_q chosen to reproduce the desired stationary
331 reservoir temperatures, 0.26 and 0.24. The *average* tempera-
332 tures, both kinetic and configurational, from the last half of a
333 400-particle, 40-million time step simulation,

334 $0 < t < 100\,000$ (equilibration);

335 $100\,000 < t < 200\,000$ (averaging),

336 are shown in Fig. 2, along with a comparison solution of the
337 macroscopic heat flow equation. The agreement is quite
338 good, as would be expected from Aoki and Kusnezov's
339 work.

340 VII. RESULTS WITH THE GAUSSIAN ISOKINETIC 341 THERMOSTAT

342 Simulations with two *Gaussian isokinetic thermostats*,
343 with the same time step, $dt=0.005$, and the same equilibra-
344 tion and averaging intervals, produced similar results, main-
345 taining the initial kinetic temperatures throughout. The aver-
346 aged profiles, along with a corresponding continuum
347 solution, are shown in Fig. 3. Again the agreement, for both
348 the kinetic and the configurational temperatures, is perfectly
349 satisfactory.

350 The instantaneous (at time t) values of the total heat
351 added (from time 0 to time t) to the “hot” reservoir as well as
352 that removed from the “cold” reservoir are shown in Fig. 4.
353 The sum of the two necessarily oscillates about zero as t
354 increases. Straight lines drawn through the data provide an
355 estimate for the Fourier conductivity in agreement with the
356 results of Aoki and Kusnezov's work. The two conventional

thermostat types, Nosé-Hoover and Gaussian isokinetic, 357
show that either method can be used to simulate the simple 358
two-temperature heat flow problem. 359

VIII. RESULTS WITH THE HOOVER-LEETE HAMILTONIAN ISOKINETIC THERMOSTAT

Results with the Hamiltonian isokinetic thermostats 362

$$\left\{ \dot{q}_{\text{Hot/Cold}} = \frac{p}{m} \sqrt{\frac{K_{\text{Hot/Cold}}}{K(p)}}; \quad \dot{p} = F(q) \right\}, \quad 363$$

where the fixed hot and cold kinetic temperatures 364
 $\langle m\dot{q}^2/k \rangle_{\text{Hot/Cold}}$ are fixed by the initial conditions, but come to 365
differ from the unconstrained momentum-based temperatures 366
 $\langle p^2/mk \rangle_{\text{Hot/Cold}}$. Unlike the Nosé-Hoover and Gaussian isoki- 367
netic profiles, the Hamiltonian-based profiles show *no tem-* 368
perature gradients at all (see Fig. 5). Instead there are dis- 369
continuities between the fixed kinetic temperatures and the 370
adjacent constant values of the unconstrained Newtonian re- 371
gions. In the latter regions the kinetic and configurational 372
temperatures equilibrate, and match the unconstrained con- 373
figurational temperature of the thermostated regions. In the 374

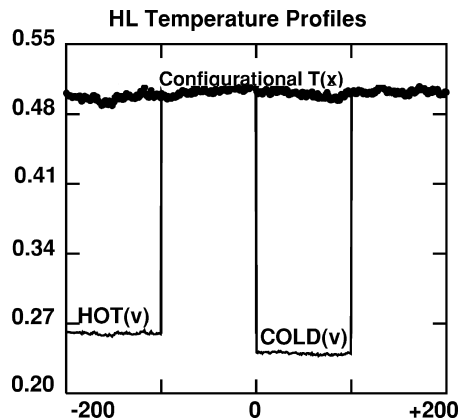


FIG. 5. Temperature profiles (kinetic and configurational) for a simulation using constrained Hoover-Leete isokinetic reservoirs. The time step is $dt = 0.005$, with a total elapsed time of 10^6 divided equally between equilibration and averaging portions. The kinetic temperature corresponds to the wiggly line; the configurational temperature to the filled circles.

375 thermostated regions there is no such equilibration.

376 Evidently there are no heat fluxes in the system either.

377 By constraining not only the energy (through the constant

378 Hamiltonian driving the motion) but also the kinetic tem-

379 peratures, the system is evidently prevented from supporting

380 heat flow. The Hamiltonian nature of the motion equations

381 also prevents the formation of the multifractal phase-space

382 distributions associated with nonequilibrium stationary

383 states.^{1,2} A more detailed analysis of the reasons for the fail-

384 ure of this Hamiltonian approach could perhaps be based on

385 a detailed analysis of the microscopic equations describing

386 heat flux.¹

387 IX. RESULTS WITH THE LANDAU-LIFSHITZ

388 HAMILTONIAN ISOCONFIGURATIONAL THERMOSTAT

389 For the special ϕ^4 model considered here, with $d=1$, the
390 force F_i is

$$391 \quad F_i = -\kappa\delta_i^3 + \mu[\delta_{i+1} - 2\delta_i + \delta_{i-1}].$$

392 The pair-potential contribution to $\nabla_i^2\mathcal{H}$ is 2μ , for the two
393 nearest-neighbor interactions

$$394 \quad \frac{\partial^2}{\partial x_i^2}(\mu/2)(|x_i - x_{i\pm 1}| - 1)^2 = \mu.$$

395 The tethering potential contribution is $3\kappa\delta_i^2 = \nabla_i^2(\kappa\delta_i^4/4)$

$$396 \quad \sum_N \nabla^2\mathcal{H} = 2N\mu + \sum_N 3\kappa\delta^2.$$

397 The time derivative of the configurational temperature is a
398 quotient of products of single-particle sums

$$399 \quad \dot{T} = \frac{2 \sum FF\dot{F}}{\sum (2\mu + 3\kappa\delta^2)} - \frac{6 \sum F^2 \sum \kappa v \delta}{\left[\sum (2\mu + 3\kappa\delta^2)\right]^2},$$

400 where

$$401 \quad \dot{F}_i = \mu[v_{i+1} - 2v_i + v_{i-1}] - 3\kappa\delta_i^2 v_i.$$

402 Another time differentiation gives the second derivative

$$413 \quad \ddot{T} = \frac{2 \sum FF\ddot{F}}{\sum (2\mu + 3\kappa\delta^2)} - \frac{6 \sum F^2 \sum \kappa v \dot{\delta}}{\left[\sum (2\mu + 3\kappa\delta^2)\right]^2} - \frac{12 \sum F \dot{F} \sum \kappa v \delta + 6 \sum F^2 (\kappa \sum [a\delta + \sum v^2])}{\left[\sum (2\mu + 3\kappa\delta^2)\right]^3},$$

$$415 \quad \lambda = \frac{\ddot{T}_{\text{Newton}}}{\sum \nabla_i T \left([2\mu(F_{i+1} - 2F_i + F_{i-1}) - 6\kappa\delta_i^2 F_i] - \left[\sum F^2 \sum 6\kappa F_i \delta_i \right] \right)}.$$

416

417

418

419 Because T cannot change, both $T=T_0$ and $\dot{T}=0$ need to be
420 properly specified in the initial conditions. A convenient way
421 to do this is to choose the velocities equal to zero so that \dot{T}
422 $\equiv 0$.

423 A typical profile using two configurational thermostats is
424 shown in Fig. 6. Just as in the Hoover-Leete isokinetic case
425 there is no equilibration of the constrained temperature (here
426 configurational). The unconstrained kinetic temperature
427 equilibrates throughout the system to a value dependent upon

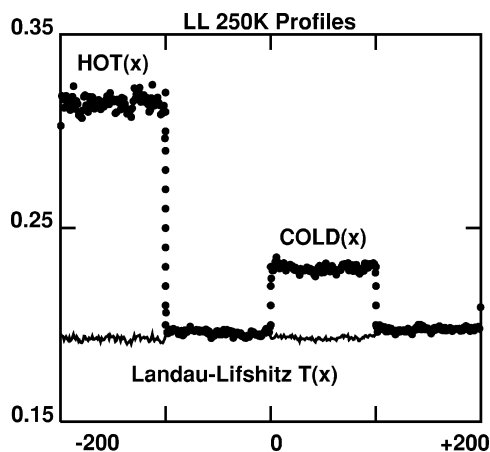


FIG. 6. Temperature profiles (kinetic and configurational) for a simulation using constrained Landau-Lifshitz isoconfigurational reservoirs. The time step is $dt=0.002$, with a total elapsed time of 500 000 divided equally between equilibration and averaging portions. The kinetic temperature corresponds to the wiggly line; the configurational temperature to the filled circles.

$$403 \quad \ddot{T}_{\text{Newton}} = \frac{2 \sum FF\ddot{F} + 2 \sum \dot{F}^2}{\sum (2\mu + 3\kappa\delta^2)} + \frac{72 \sum F^2 \left[\sum \kappa v \delta \right]^2}{\left[\sum (2\mu + 3\kappa\delta^2) \right]^3}$$

$$404 \quad - \frac{24 \sum FF\dot{F} \sum \kappa v \delta + 6 \sum F^2 (\kappa \sum [a\delta + \sum v^2])}{\left[\sum (2\mu + 3\kappa\delta^2) \right]^2},$$

where

$$406 \quad \ddot{F}_i = \mu[a_{i+1} - 2a_i + a_{i-1}] - \kappa[3\delta_i^2 a_i + 6\delta_i v_i^2].$$

The second derivative, \ddot{T} , introduces the Lagrange multiplier
407 through the equations of motion

$$409 \quad \{a_i = \dot{v}_i = F_i - \lambda \nabla_i T\}.$$

410 Though complicated, the resulting equation for λ is linear,
411 and gives an explicit expression for the Lagrange multiplier
412 that stabilizes T

428 the initial conditions. Evidently the Landau-Lifshitz con-
429 strained configurational thermostat is quite useless for non-
430 equilibrium work.

431 X. CONCLUSIONS

432 The results obtained with the Gaussian isokinetic and
433 Nose-Hoover thermostats are quite consistent with the past
434 history of their use over the last quarter century.^{1,2,6,7} For
435 these familiar thermostats there was no problem in reaching

436 a nonequilibrium steady state with temperature profiles and
 437 heat fluxes very similar to those expected from macroscopic
 438 hydrodynamics using Fourier's law. Although the simple ϕ^4
 439 model may strike the reader as rather special we believe that
 440 the results obtained using it are *typical* of realistic applica-
 441 tions. The lack of momentum conservation in this model, due
 442 to the tethering potential, though it certainly eliminates the
 443 low-frequency divergence of the one-dimensional heat con-
 444 ductivity, actually makes the one- and two-dimensional mod-
 445 els more closely resemble their *more physical* three-
 446 dimensional cousins. We expect that the configurational
 447 analog¹⁴ of the Nosé-Hoover kinetic thermostat, discussed in
 448 Sec. II, would provide very similar results. It would be par-
 449 ticularly interesting to explore the differences between the
 450 tensor forms of the kinetic and configurational temperatures,
 451 by applying these ideas to strong shockwaves.

452 On the other hand, the results obtained with *purely*
 453 *Hamiltonian* mechanics, using either the Hoover-Leete con-
 454 strained isokinetic or the Landau-Lifshitz constrained con-
 455 figurational thermostats were both unexpected and thought-
 456 provoking. The main message of the current work is that
 457 unadulterated Hamiltonian mechanics is simply unsuitable to
 458 steady-state nonequilibrium simulations. The longtime re-
 459 sults, using Hamiltonian mechanics, are tied to both the en-
 460 ergy and the phase volume of the initial conditions, in a way
 461 simply inconsistent with the known phase-space contraction
 462 typical of nonequilibrium systems. From the aesthetic stand-
 463 point, we believe that the canonical-ensemble derivations of
 464 Landau and Lifshitz¹² and Travis and Braga¹⁴ are not only
 465 clearer, but also more useful and stimulating than is Rugh's
 466 alternative microcanonical approach.¹³

467 Both the Hamiltonian approaches stably constrained
 468 their target temperatures in the two reservoir regions. Never-
 469 theless temperature differences led to no net heat flow and
 470 the computed temperature profiles bore no resemblance to
 471 the predictions of hydrodynamics. The kinetic and configu-
 472 rational temperatures, though *unequal* in the constrained res-
 473 ervoirs

$$474 \quad T_{\text{kin}} \neq T_{\text{con}} [\text{reservoirs}],$$

475 *were* equal (to yet a third nearly constant temperature) in the
 476 unconstrained bulk Newtonian regions

$$T_{\text{kin}} = T_{\text{con}} [\text{bulk}]. \quad 477$$

These results emphasize the fact that *nonHamiltonian* dy- 478
 namics is absolutely necessary to the realistic modeling of 479
 nonequilibrium systems. A direct proof/understanding of the 480
 failure of the Hamiltonian systems to show a nonvanishing 481
 heat flux would be most welcome. 482

ACKNOWLEDGMENTS 483

This work was first presented at a Mexico City work- 484
 shop organized by Francisco Uribe at Universidad Autónoma 485
 Metropolitana-Iztapalapa in January, 2007. Subsequently, a 486
 shorter version was presented at the Schrödinger Institute 487
 workshop, in Wien, 18–20 April 2007, honoring the 65th 488
 birthday of Herr Professor Doktor Harald Posch. We are es- 489
 pecially grateful to Professors Uribe, Posch, and Dellago for 490
 making this work possible. Brad Holian and Janka Petracic 491
 kindly commented on an earlier version of this paper. Karl 492
 Travis provided us with copies of Refs. 14–16. 493

- ¹Wm. G. Hoover, *Computational Statistical Mechanics* (Elsevier, New 494
York, 1991). 495
- ²Wm. G. Hoover, *Computer Simulation, Time Reversibility, and Chaos* 496
(World Scientific, Singapore, 1999 and 2001). 497
- ³W. T. Ashurst and W. G. Hoover, *Phys. Rev. Lett.* **31**, 206 (1973). 498
- ⁴C. P. Dettmann and G. P. Morriss, *Phys. Rev. E* **54**, 2495 (1996). 499
- ⁵D. J. Evans, W. G. Hoover, B. H. Failor, and B. Moran, *Phys. Rev. A* **28**, 500
1016 (1983). 501
- ⁶W. G. Hoover, *Physica* **118A**, 111 (1983).0031-8914 502
- ⁷W. G. Hoover, *Physica* **240A**, 1 (1997).0031-8914 503
- ⁸T. M. Leete, "The Hamiltonian Dynamics of Constrained Lagrangian 504
Systems," M.S. thesis, West Virginia University, 1979. 505
- ⁹S. Nosé, *Prog. Theor. Phys. Suppl.* **103**, 1 (1991). 506
- ¹⁰L. V. Woodcock, *Chem. Phys. Lett.* **10**, 257 (1971). 507
- ¹¹W. T. Ashurst, "Dense Fluid Shear Viscosity and Thermal Conductivity 508
via Nonequilibrium Molecular Dynamics," Ph.D. dissertation, University
of California at Davis/Livermore, 1974. 509
- ¹²L. D. Landau and E. M. Lifshitz, *Statistical Physics* (McGraw-Hill, New 511
Jersey, 1958), Eq. 33.14. 512
- ¹³J. G. Powles, G. Rickayzen, and D. M. Heyes, *Mol. Phys.* **103**, 1361 513
(2005).0026-8976 514
- ¹⁴C. Braga and K. P. Travis, *J. Chem. Phys.* **123**, 134101 (2005). 515
- ¹⁵C. Braga and K. P. Travis, *J. Chem. Phys.* **124**, 104102 (2006). 516
- ¹⁶K. P. Travis and C. Braga, *Mol. Phys.* **104**, 3735 (2006).0026-8976 517
- ¹⁷K. Aoki and D. Kusnezov, *Phys. Lett. B* **477**, 348 (2000). 518
- ¹⁸K. Aoki and D. Kusnezov, *Phys. Lett. A* **309**, 377 (2003). 519